# Chapter 7

# Thermopower of single molecules

## 7.1 Introduction

In this chapter, we investigate the thermopower of single-molecule devices. The thermopower is defined as the ratio of bias voltage $V$ and an applied temperature difference $\Delta T$ under the condition that the current vanishes:

$$S = -\lim_{\Delta T \to 0} \frac{V}{\Delta T}\bigg|_{I=0}. \tag{7.1}$$

A very interesting feature of the thermopower is that, unlike the $IV$ characteristic, it provides information on whether the current flow proceeds predominantly through the LUMO or HOMO. The underlying reason is that a nonzero thermopower requires breaking of particle-hole symmetry about the Fermi energy. For quantum dots the thermopower for pure sequential tunneling has been investigated theoretically by Beenakker and Staring [116] and experimentally by Staring et al. [117]. The cotunneling regime [86] and the crossover have been studied by Turek and Matveev [88]. In the case of a quantum dot strongly coupled to one lead, the thermopower has been investigated by Matveev and Andreev [118].

Here, we extend these considerations to transport through single molecules, where experimental work [26, 28, 29] indicates that phonons may play an important role. We base our calculations on the Anderson-Holstein Hamiltonian, Eqs. (1.1)–(1.3), slightly going beyond the model introduced in Chapter 1 by considering both internal vibrations as well as CM oscillations of the molecule. Employing the rate-equation approach valid for weak molecule-lead coupling (see Chapter 2), we compute the thermopower as a function of gate voltage, temperature, and electron-phonon coupling.

We find that the sign of the thermopower reveals whether transport is dominated by electrons or holes. Moreover, the thermopower contains information on the electronic and phononic excitations of the molecule. This way of measuring the molecular excitations in linear response [cf. the $\Delta T \to 0$ limit in Eq. (7.1)] may have advantages over the more conventional $IV$ characteristic. The latter necessarily involves nonequilibrium effects, which may be difficult to interpret. Moreover, a large applied voltage may even affect symmetry and structure of the molecule itself.

To leading order perturbation theory for the molecule-lead coupling (sequential-tunneling contributions), we find that the thermopower as a function of gate voltage develops a saw-

tooth behavior in the low temperature limit with steps due to electronic and phononic excitations. Step sizes and their dependence on the electron-phonon coupling strength are analyzed.

Going beyond the sequential approximation, we find that in a wide range of parameters cotunneling contributions from next-to-leading order perturbation theory in the tunneling are important.[1] We investigate these contributions and the full crossover between the sequential-tunneling and the cotunneling regimes. We find that elastic cotunneling does not show any significant phonon structure, and discuss under which conditions phonon features due to sequential-tunneling are retained in the total thermopower.

The outline of this chapter is as follows: Section 7.2 describes a generalization of the Anderson-Holstein, which includes molecular CM oscillations. Our calculations for the thermopower are described in Section 7.3 and the results are presented in Section 7.4. We summarize our findings in Section 7.5. Some calculational details including the results of the cotunneling regularization are relegated to appendices.

## 7.2 Extended Model

In extension to the Anderson-Holstein model of Chapter 1, we here distinguish two types of phonons, which we term vibrations and oscillations: Vibrations are internal phonon modes of the molecule, for which the center of mass (CM) of the molecule is at rest, and which are incorporated in the Hamiltonian Eq. (1.1). On the other hand, oscillations involve movement of the molecule as a whole, which has been observed in experiments with physisorbed[2] molecules [26]. To describe oscillations, we introduce the momentum and position operators $p_z$ and $z$ of the CM displacement. In the case of physisorption the coupling to the leads is weak, so that the two phonon types typically involve different energy scales: Vibrations, which are associated with strong intra-molecular bonds, will have considerably higher energies than oscillations. The two phonon types also differ in the nature of coupling: Vibrations directly couple to the electric charge on the molecule, described by the term $\sim n_d(b^\dagger + b)$, whereas the coupling for oscillations occurs through displacement-dependent tunneling matrix elements $t_{L,R}(z)$.

Specifically, the displacement dependence of the tunneling matrix elements for oscillations is obtained by the following consideration. The tunneling matrix element $t$ describes the tunneling processes between the leads and the molecule, and we may assume an exponential fall-off of $t$ with increasing distance between lead and molecule. For a symmetric molecule of length $2l$ between two leads with a separation distance $2d$, this yields

$$t_{L,R}(z) = t_0 \exp[-(d - l \pm z)/z_0]. \tag{7.2}$$

[1] At low temperatures the cotunneling terms increase due to higher order contributions that lead to strong Kondo correlations near the Kondo temperature $T_K$. Here, we assume temperatures high compared to the Kondo temperature, $T \gg T_K$. The thermopower for $T \gtrsim T_K$ can be estimated by substituting the cotunneling rate by an effective one, which is renormalized by the higher-order terms, cf., e.g., M. Pustilnik and L. I. Glazman, J. Phys. Condens. Matter **16**, R513 (2004).

[2] Physisorption refers to weak bonding of a molecule to a surface by van-der-Waals forces or hydrogen bridge bonds, as opposed to chemisorption, which terms the case of strong covalent bonds between molecule and surface.

The parameter $z_0$ fixes the length scale of the exponential fall-off of the electronic wave functions outside the leads and the molecule. In the following, we restrict ourselves to considering one phonon type at a time. Whenever the specific phonon type is irrelevant we will skip the subscripts "vib" and "osc".

## 7.3 Thermopower

The thermopower, Eq. (7.1), is calculated by considering the current through the molecule in the linear response regime, which is

$$I(V, \Delta T) = GV + G_T \Delta T + \mathcal{O}(V^2, \Delta T^2, V\Delta T), \tag{7.3}$$

where $G$ denotes the conductance, $G_T$ the thermal coefficient, and $\Delta T = T_L - T_R$ the temperature difference between the left and right lead. Hence, the thermopower can be written as

$$S = \frac{G_T}{G} = \frac{G_T^{\mathrm{sq}} + G_T^{\mathrm{co}}}{G^{\mathrm{sq}} + G^{\mathrm{co}}}, \tag{7.4}$$

where sequential tunneling and cotunneling contributions have been separated. We investigate both contributions to the thermopower and obtain expressions valid in the full crossover regime by means of the regularization scheme for cotunneling rates (Appendix C).

In order to obtain the conductance $G$ and the thermal linear-response coefficient $G_T$, we expand the current (2.16) in the bias voltage $V = V_L - V_R$ and the temperature difference $\Delta T = T_L - T_R$. Since $V$ and $\Delta T$ are in principle infinitesimal, we can conveniently choose the right electrode to have zero potential and temperature $T$. Accordingly, the left electrode has potential $V$ and temperature $T + \Delta T$. When expanding the current, one has to expand both the probabilities $P_q^n$ and the transition rates $W_{qq'}^{nn'}$.

We write the expansion for the transition rates and probabilities as

$$W_{qq'}^{nn'} = w_{qq'}^{nn'} + \Delta T\, t_{qq'}^{nn'} + V\, v_{qq'}^{nn'} + \cdots \tag{7.5}$$

and

$$P_q^n = \overline{P_q^n} + \Theta_q^n \Delta T + \Phi_q^n\, V + \cdots . \tag{7.6}$$

Here, $\overline{P_q^n} = 2^{\delta_{1,n}} \exp(-E_q^n/k_BT)/Z$ denotes the grandcanonical probability distribution at equilibrium, and $Z = \sum_{n,q} 2^{\delta_{1,n}} \exp(-E_q^n/k_BT)$ the corresponding partition function.[3] The normalization condition for the deviations of $P_q^n$ from its equilibrium value is $0 = \sum_{n,q} \Theta_q^n = \sum_{n,q} \Phi_q^n$.

By substituting the expansions (7.5), (7.6) into the rate equations (2.9) and retaining only terms linear in $V$ and $\Delta T$, one obtains a new set of rate equations for the deviations $\Theta_q^n$ and $\Phi_q^n$, see Appendix K, Eq. (K.1). These, in conjunction with the normalization conditions for $\Theta$ and $\Phi$, represent an inhomogeneous system of linear equations, whose solution yields the deviations $\Theta_q^n$ and $\Phi_q^n$. Finally, the current (G.5) can be expanded in

[3] The additional factor of $2^{\delta_{n,1}}$ takes into account the spin-degeneracy of the level $n = 1$.

terms of $\Delta T$ and $V$:

$$I = \sum_{n,q,q'} (\Delta T \Theta_q^n + V \Phi_q^n) \left[ w^{n,n+1}_{qq';\,R} - w^{n,n-1}_{qq';\,R} \right] + \sum_{n,q,q'} \overline{P_q^n} \Big[ \Delta T (t^{nn}_{qq';\,RL} - t^{nn}_{qq';\,LR}) + V (v^{nn}_{qq';\,RL} - v^{nn}_{qq';\,LR}) \Big] \tag{7.7}$$

Note that the terms proportional to $\Theta_q^n$ and $\Phi_q^n$ in the expansion of the cotunneling contributions are absent since the rates of cotunneling from left to right and vice versa cancel each other at zero bias, $(w^{nn}_{qq';\,RL} - w^{nn}_{qq';\,LR}) = 0$.

### 7.3.1 Sequential-tunneling contributions

In Eq. (7.7) it was chosen to expand $I_R$ in $V$ and $\Delta T$. Due to the steady-state property $I = I_R = I_L$, an expansion in $I_L$ gives the same result and it turns out to be convenient to expand the expression $I = (I_L + I_R)/2$, which for the sequential-tunneling contributions results in

$$\begin{aligned} I^{\mathrm{sq}} =& \frac{1}{2} \sum_{n,q,q'} (\Delta T \Theta_q^n + V \Phi_q^n) \left[ w^{n,n+1}_{qq';\,R} - w^{n,n-1}_{qq';\,R} + w^{n,n-1}_{qq';\,L} - w^{n,n+1}_{qq';\,L} \right] \\ &+ \frac{1}{2} \sum_{n,q,q'} \overline{P_q^n} V \left[ v^{n,n-1}_{qq';\,L} - v^{n,n+1}_{qq';\,L} \right] + \frac{1}{2} \sum_{n,q,q'} \overline{P_q^n} \Delta T \left[ t^{n,n-1}_{qq';\,L} - t^{n,n+1}_{qq';\,L} \right]. \end{aligned} \tag{7.8}$$

Here, the first term remarkably vanishes due to the symmetry[4] $w^{n,n\pm1}_{qq';\,R} = w^{n,n\pm1}_{qq';\,L}$. Therefore, one obtains the following sequential-tunneling contributions to the thermal coefficient $G_T$ and the conductance $G$,

$$G_T^{\mathrm{sq}} = \frac{1}{2} \sum_{n,q,q'} \overline{P_q^n} \left[ t^{n,n-1}_{qq';\,L} - t^{n,n+1}_{qq';\,L} \right], \qquad G^{\mathrm{sq}} = \frac{1}{2} \sum_{n,q,q'} \overline{P_q^n} \left[ v^{n,n-1}_{q\to q';\,L} - v^{n,n+1}_{qq';\,L} \right]. \tag{7.9}$$

We point out that the so-obtained conductance and thermal coefficient do not depend on the probability deviations $\Theta_q^n$ and $\Phi_q^n$ any more. This is an important result since it allows for an analytic expression of the thermopower not involving an explicit solution of the rate equations, cf. Appendix K. [Expansions of $I_L$ and $I_R$ alone lead to expressions for $G^{\mathrm{sq}}$ and $G_T^{\mathrm{sq}}$, which do involve $\Theta_q^n$ and $\Phi_q^n$. We have also carried out calculations based on this approach by solving the rate equations for the probability deviations and find agreement with the results from Eq. (7.9).]

### 7.3.2 Cotunneling contributions

The cotunneling contributions to thermal coefficient and conductance are

$$G_T^{\mathrm{co}} = \sum_{n,q,q'} \overline{P_q^n} \left[ t^{nn}_{qq';\,RL} - t^{nn}_{qq';\,LR} \right], \qquad G^{\mathrm{co}} = \sum_{n,q,q'} \overline{P_q^n} \left[ v^{nn}_{qq';\,RL} - v^{nn}_{qq';\,LR} \right]. \tag{7.10}$$

[4] This symmetry is a consequence of the fact that the rates $w$ are evaluated at *zero bias*.

In principle, any set of rate equations involving phononic excitations yields an infinite system of linear equations. In numerical calculations one makes use of the fact that transitions involving highly excited phonon states typically result in small rates. This allows for the introduction of a cutoff phonon number.

We find that the linear response quantities $G$ and $G_T$ do not depend on the relaxation time $\tau$. Mathematically, this corresponds to the result that the conductance and thermal coefficient do not involve the probability deviations $\Phi_q^n$ and $\Theta_q^n$, cmp. Eqs. (7.9)–(7.10). The physical reason for this is the following: In the $I \to 0$ limit, the average time needed for one electron tunneling through the molecule becomes large compared to the relaxation time. Consequently, the initial state for any tunneling process corresponds to an equilibrium phonon state.

By substituting back Eqs. (7.9)–(7.10) into Eq. (7.4), we arrive at the following analytical expression for the thermopower:

$$S = \frac{\sum_{n,q,q'} \overline{P_q^n} \left[ t^{n,n-1}_{qq';\,L} - t^{n,n+1}_{qq';\,L} + 2t^{nn}_{qq';\,RL} - 2t^{nn}_{qq';\,LR} \right]}{\sum_{n,q,q'} \overline{P_q^n} \left[ v^{n,n-1}_{qq';\,L} - v^{n,n+1}_{qq';\,L} + 2v^{nn}_{qq';\,RL} - 2v^{nn}_{qq';\,LR} \right]}. \tag{7.11}$$

This equation is our central result. It shows that even in the presence of phonons, the thermopower can be expressed analytically through the equilibrium probability distribution $\overline{P_q^n}$ and the expansion coefficients of the transition rates evaluated at vanishing source drain voltage and temperature difference. In the following section the implications of Eq. (7.11) will be discussed.

## 7.4 Results

### 7.4.1 Sequential tunneling

We first consider the results for pure sequential tunneling, postponing the discussion of the full thermopower due to both sequential and cotunneling to Sec. 7.4.2. We give numerical results for the thermopower and present analytic expressions for the limiting case $U \to \infty$ and $T \to 0$ below. Representative numerical results are shown in Fig. 7.1.

The dominant feature of the sequential-tunneling thermopower $S^{\mathrm{sq}}$ is a large step at the gate voltage $\varepsilon_d^* = -U/2$, for which the Fermi energy of the leads lies halfway in between the $|\,1,0\,\rangle$ and the $|\,2,0\,\rangle$ state. This situation is depicted in Fig. 7.2. At $\varepsilon_d = \varepsilon_d^*$ the thermocurrent $G_T \Delta T$ vanishes due to electron-hole symmetry. An increased (decreased) gate voltage lowers (raises) the molecular levels with respect to the Fermi level, and therefore current is dominated by electrons (holes) flowing from the left to the right lead. Consequently, $G_T$ changes sign at $\varepsilon_d = \varepsilon_d^*$. Moreover, away from the Coulomb peaks, sequential tunneling can only occur through the tails of the lead Fermi distributions due to energy conservation. Therefore, the sequential-tunneling conductance and thermal coefficient fall off exponentially away from the Coulomb peak. At gate voltages close to $\varepsilon_d^*$, their behavior can be estimated by

$$G^{\mathrm{sq}} \sim \exp[\varepsilon_d^*/k_BT] \cosh[(\varepsilon_d^* - \varepsilon_d)/k_BT], \tag{7.12}$$

$$G_T^{\mathrm{sq}} \sim \exp[\varepsilon_d^*/k_BT] \sinh[(\varepsilon_d^* - \varepsilon_d)/k_BT]. \tag{7.13}$$

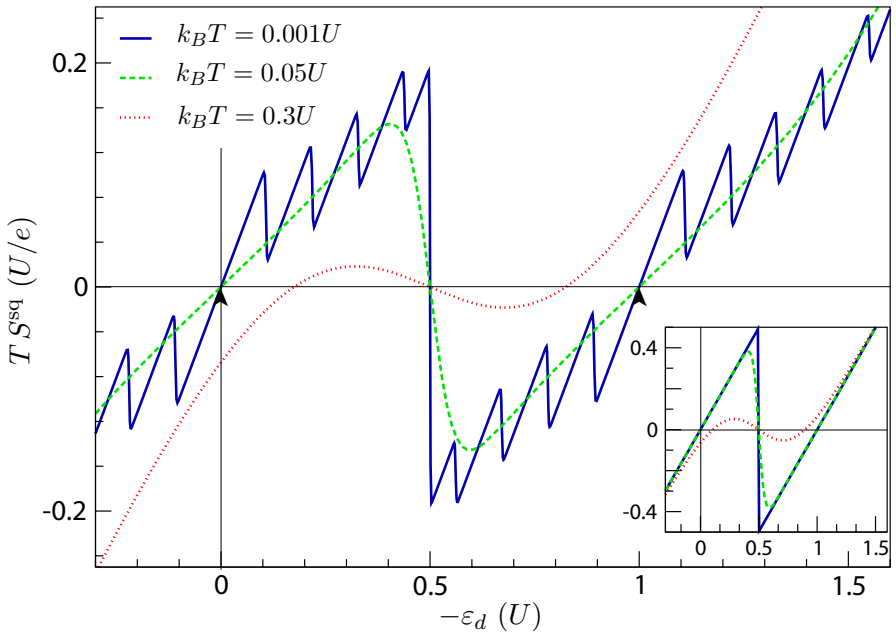


**Figure 7.1**: Thermopower $S^{\rm sq}$ times temperature as a function of gate voltage for $\hbar\omega_0 = 0.11U$. Large: Vibrations with $\lambda = 2$. Inset: Oscillations with $\xi_0 = 5$. (See text below Eq. (7.16) for a discussion of the choice of parameters.) The positions of the corresponding Coulomb peaks in $\partial I/\partial V$ are marked with arrows. In contrast, the main features of the thermopower occur between the Coulomb peaks.

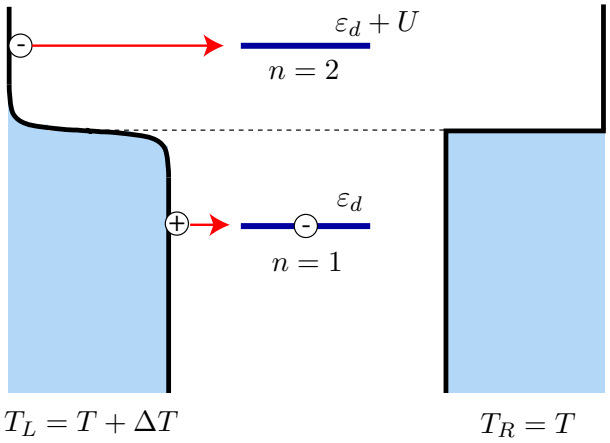


**Figure 7.2**: Electron-hole symmetry for the gate voltage $\varepsilon_d = -U/2$.

Consequently, the sequential-tunneling thermopower $S^{\mathrm{sq}} = G_T^{\mathrm{sq}}/G^{\mathrm{sq}}$ behaves as $\sim \tanh[(\varepsilon_d^* - \varepsilon_d)/k_BT]$ in the vicinity of $\varepsilon_d^*$, which develops a discontinuity in the limit $T \to 0$.

In addition to the electronic step, the results show smaller phonon steps with a distance of $\hbar\omega_0$ between adjacent steps. To understand slope, temperature dependence, and phonon step sizes of the sequential-tunneling thermopower, we turn to the case $U \to \infty$. In this limit, electronic double occupation of the molecule is forbidden, and the sequential-tunneling thermopower $S^{\mathrm{sq}} = G_T^{\mathrm{sq}}/G^{\mathrm{sq}}$ reads

$$\begin{aligned} S^{\mathrm{sq}} &= \frac{\sum_{q,q'} P_q^{\mathrm{eq}}(\overline{P^0}t_{qq'}^{01} - \overline{P^1}t_{qq'}^{10})}{\sum_{q,q'} P_q^{\mathrm{eq}}(\overline{P^0}v_{qq'}^{01} - \overline{P^1}v_{qq'}^{10})} \\ &= -\frac{\varepsilon_d}{eT} - \frac{\sum_{q,q'}(\overline{P^0}P_q^{\mathrm{eq}} + \overline{P^1}P_{q'}^{\mathrm{eq}}) f'(E_{q'}^1 - E_q^0)\hbar\omega_0(q'-q)\left|M_{q'\to q}\right|^2}{eT\sum_{q,q'}(\overline{P^0}P_q^{\mathrm{eq}} + \overline{P^1}P_{q'}^{\mathrm{eq}}) f'(E_{q'}^1 - E_q^0)\left|M_{q'\to q}\right|^2}. \end{aligned} \tag{7.14}$$

Here, we have used that the equilibrium distribution $\overline{P_q^n}$ factorizes into an electronic and a phononic part, with the latter given by $P_q^{\mathrm{eq}} = e^{-q\hbar\omega_0/k_BT}(1 - e^{-\hbar\omega_0/k_BT})$. Thus, we find that the thermopower purely due to sequential tunneling roughly scales like $1/T$, which is in agreement with the quantum dot case [116]. In the low temperature limit, the thermopower develops a characteristic sawtooth behavior as a function of gate voltage. The slope of the linear pieces is found to be $dS^{\mathrm{sq}}/d\varepsilon_d = -1/eT$.

In the $T \to 0$ limit, one obtains

$$\lim_{T\to 0} TS^{\mathrm{sq}} = -\frac{\varepsilon_d}{e} + \mathrm{sgn}(\varepsilon_d)\frac{\sum_{q<|\varepsilon_d|/\hbar\omega_0} q\hbar\omega_0\left|M_{0q}\right|^2}{e\sum_{q<|\varepsilon_d|/\hbar\omega_0}\left|M_{0q}\right|^2}, \tag{7.15}$$

where the last term generates the step features by adding up higher phonon contributions for increasing gate voltages. We can obtain the phononic step size $\Delta_Q$ of the $Q$th step of $TS^{\mathrm{sq}}$ in the $T \to 0$ limit from Eq. (7.15),

$$\Delta_Q = \frac{\hbar\omega_0}{e}\left|M_{0Q}\right|^2\sum_{q=0}^{Q}(Q-q)\left|M_{0q}\right|^2\left[\sum_{q=0}^{Q}\left|M_{0q}\right|^2\sum_{q=0}^{Q-1}\left|M_{0q}\right|^2\right]^{-1}. \tag{7.16}$$

Here, $Q$ counts the discontinuities of $TS^{\mathrm{sq}}$ starting at $\varepsilon_d = 0$ with increasing gate voltage. $\Delta_Q$ depends on the step number $Q$ and on the coupling strength $\lambda$ or $\xi_0 = z_0/\ell_{\mathrm{osc}}$ for vibrations or oscillations, respectively. Here, $\ell_{\mathrm{osc}} = (\hbar/M\omega_{\mathrm{osc}})^{1/2}$ is the harmonic-oscillator length for oscillations and $M$ denotes the molecular mass.

It is instructive to estimate typical values of the parameters $\xi_0$ and $\lambda$ for realistic systems. For $\xi_0$ we need to compare $z_0$ to the oscillator length $\ell_{\mathrm{osc}}$. An order of magnitude estimate yields $z_0 \approx \hbar/(m_eW)^{1/2}$. Here, $W$ is the work function of the metal leads and is of the order of several eV. On the other hand, for a typical experiment [26] oscillations occur on an energy scale of 1–10 meV. This yields $\xi_0 = z_0/\ell_{\mathrm{osc}} \gg 1$. In this case, displacements of the molecule's CM are small on the scale of $z_0$, and therefore no significant shuttle effects [75,76] can be expected.

Next we consider the vibrational coupling parameter $\lambda$. Let $r$ be the normal coordinate deviation from the equilibrium value $r_0$. To leading order, charging the molecule with an

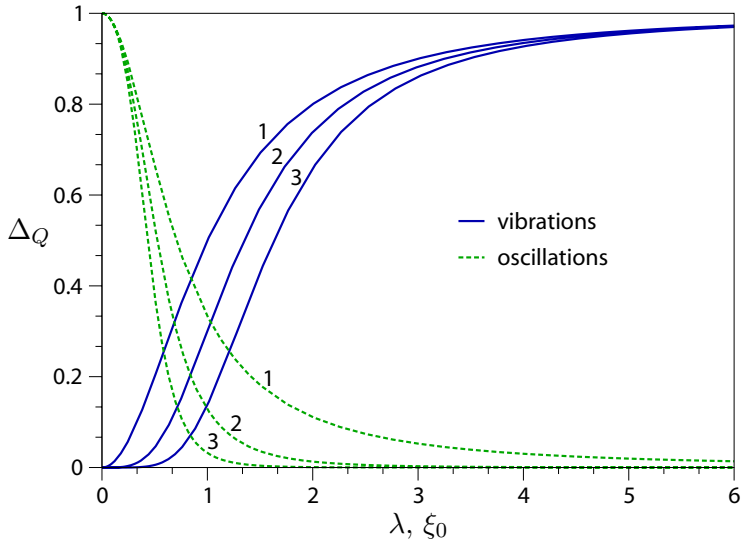


**Figure 7.3**: Phonon step size $\Delta_Q$ in units of $\hbar\omega_0/e$ for the step numbers $Q = 1, 2, 3$.

additional electron has the effect of shifting the phonon potential curve by some distance $\Delta r$, so that the potential energy is now $\approx \frac{1}{2}M\omega_{\rm vib}^2(r + n\Delta r)^2$. Hence, the electron-phonon coupling term is of the order of magnitude of $M\omega_{\rm vib}^2 r\Delta r = \Delta r/\ell_{\rm vib}\hbar\omega_{\rm vib}(b{+}b^\dagger)$ and therefore $\lambda \approx \Delta r/\ell_{\rm vib}$. Here, $\ell_{\rm vib} = (\hbar/M\omega_{\rm vib})^{1/2}$ is the harmonic oscillator length corresponding to vibrations. There is not a general rule for how $\ell_{\rm vib}$ and $\Delta r$ compare so that $\lambda$ can in principle assume values both smaller and larger than 1.

Due to the different behavior of the matrix elements for vibrations and oscillations, the phonon step size turns out to differ between those two cases as shown in Fig. 7.3. For vibrational phonons, the electron-phonon coupling becomes stronger for increasing $\lambda$. In the case of electron-phonon coupling for oscillations, the coupling gets stronger for decreasing $\xi_0 = z_0/\ell_{\rm osc}$.[5] Thus, the plausible finding is that in both cases phonon step size increases with the effective electron-phonon coupling strength. For oscillations the steps are rather small in the relevant regime of $\xi_0 \gg 1$. For vibrations they may be more pronounced.

### 7.4.2 Results for the total thermopower

The results for the thermopower discussed above arise from considering sequential-tunneling contributions only. However, if the Fermi levels are not aligned with a molecular level, sequential tunneling only occurs via electrons (or holes) in the tails of the Fermi distributions in the leads. In this case, the sequential-tunneling conductance $G^{\rm sq}$ and thermal coefficient $G_T^{\rm sq}$ are exponentially suppressed, and higher-order processes such as cotunneling may yield important contributions. Accordingly, sequential tunneling dominates in proximity to the

[5] Decreasing $z_0$ at fixed $\ell_{\rm osc}$ increases the position dependence of the hopping matrix elements $t(z)$.

aligned-levels configuration, and is suppressed most at the gate voltage $\varepsilon_d^*$ at which the large electronic step in the sequential-tunneling thermopower occurs. In the latter range of gate voltages, cotunneling may give the dominant contributions to the thermopower. For this reason we have included the effect of cotunneling processes in the rate-equations approach. At temperatures $k_BT < \hbar\omega_0$, inelastic cotunneling can be neglected, and we find that the elastic cotunneling does not exhibit significant phonon structure.

Figure 7.4(a) exemplifies the behavior of the thermopower including both sequential and cotunneling as a function of gate voltage for several temperatures. Whether the total thermopower $S$ shows the sequential-tunneling phonon structure or whether it is mainly dominated by cotunneling contributions without significant phonon features, strongly depends on the choice of parameters. Firstly, step-like features can only be expected if the sequential-tunneling part develops pronounced steps. As discussed above, this depends on phonon type, phonon-coupling strength, and temperature. Only for temperatures well below $\hbar\omega_0/k_B$ one can expect any features, as can be seen from the smoothening of the phonon steps for increasing temperature in Fig. 7.4(a). Secondly, temperature and the dimensionless coupling parameter,

$$\alpha = \rho \left|t_a\right|^2 / U, \tag{7.17}$$

which arises in the rate equations and roughly describes the relative strength of cotunneling to sequential tunneling,[6] determine where the crossover between the sequential-tunneling and cotunneling regimes occurs. For illustration, Fig. 7.4(b) shows the thermopower $S$ as a function of gate voltage at fixed temperature for two different coupling parameters $\alpha$ as well as the corresponding sequential-tunneling result for comparison.

The crossover between the sequential-tunneling and cotunneling regimes occurs in a rather small gate-voltage range, cf. Fig. 7.4(a) and (b), which allows one to identify crossover gate voltage $\varepsilon_d^{\mathrm{xo}}$.[7] Our results show that the crossover points roughly scale as $\varepsilon_d^{\mathrm{xo}} \sim T \ln \alpha^{-1}$, which is in agreement with corresponding results for quantum dots, cf., e.g., Ref. [88].

This can be understood based on the following estimate of the crossover points $\varepsilon_d^{\mathrm{xo}}$. We assume that only a small gate-voltage region is dominated by sequential tunneling, $|\varepsilon_d^{\mathrm{xo}}| < |\varepsilon_d^*|$. With $\Delta\varepsilon_d = \min_{m=0,1} |\varepsilon_d + mU|$ being the dominant activation energy for either electrons or holes, one can roughly estimate the sequential-tunneling conductance and thermal coefficient by an activated behavior dependence,

$$G^{\mathrm{sq}}, G_T^{\mathrm{sq}} \sim \exp(-\Delta\varepsilon_d / k_BT). \tag{7.18}$$

While sequential-tunneling contributions therefore fall off exponentially with $\Delta\varepsilon_d$, cotunneling contributions only show a weak power-law dependence on the activation energy $\Delta\varepsilon_d$, and temperature $T$. To lowest order they may be approximated by a constant,

$$G^{\mathrm{co}}, G_T^{\mathrm{co}} \sim \alpha b. \tag{7.19}$$

Comparison of equations (7.18) and (7.19) yields as an estimate for the crossover gate voltage

$$\varepsilon_d^{\mathrm{xo}} \approx -k_BT(\ln \alpha^{-1} - \ln b). \tag{7.20}$$

[6] In this chapter, we measure the sequential and cotunneling rates in natural units of $\rho \left|t_a\right|^2 / \hbar$ and $\rho^2 \left|t_a\right|^4 / (\hbar^2 U)$, respectively.

[7] Strictly speaking, the crossover "point" is a region, and can be slightly different for $G$ and $G_T$.

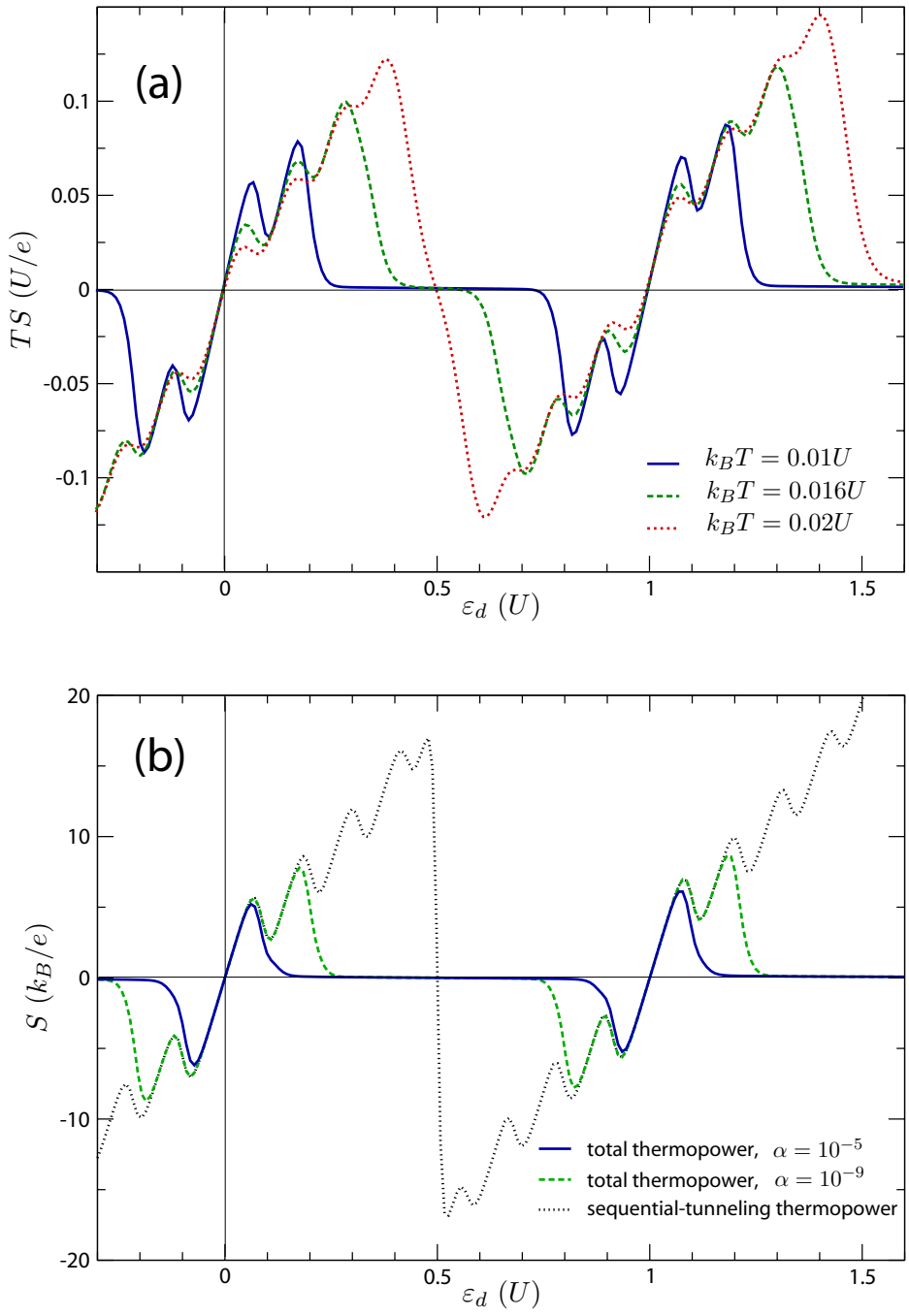


**Figure 7.4**: (a) Thermopower times temperature as a function of gate voltage for several temperatures. The parameter choices are: $\hbar\omega_0 = 0.11U$, $\lambda = 2$ (vibrations), $\alpha = 10^{-9}$ (dimensionless coupling parameter defined in Eq. (7.17)). (b) Thermopower as a function of gate voltage at fixed temperature. The parameter choices are: $\hbar\omega_0 = 0.11U$, $\lambda = 2$ (vibrations), $T = 0.01U/k_B$.

In this approximation, $|\varepsilon_d^{\mathrm{xo}}|$ increases linearly with temperature and decreases logarithmically like $\ln \alpha^{-1}$. The number of phonon steps (if present in the sequential-tunneling contribution) is given by $|\varepsilon_d^{\mathrm{xo}}| / \hbar\omega_0$.

For the parameter choices of Fig. 7.4(b), we find that $b$ assumes values which allow us to neglect the $\ln b$ term in Eq. (7.20). This leads to the following estimates of the crossover gate voltage: $\varepsilon_d^{\mathrm{xo}} \approx -0.1U$ for $\alpha = 10^{-5}$, and $\varepsilon_d^{\mathrm{xo}} \approx -0.2U$ for $\alpha = 10^{-9}$, which is in good agreement with the crossovers observed in Fig. 7.4(b).

We note that the thermopower attains rather small values in the cotunneling regime. This is plausible when reconsidering the effect of the electron-hole symmetry at $\varepsilon_d^* = U/2$. Due to this symmetry, the thermopower must vanish at $\varepsilon_d^*$. In the case of sequential tunneling, the exponentially suppressed current $G_T^{\mathrm{sq}} \Delta T$ shows the breaking of this symmetry for small gate voltage deviations from $\varepsilon_d^*$ rather abruptly (leading to the large steps in the sequential-tunneling thermopower $S^{\mathrm{sq}}$ as a function of gate voltage). For cotunneling on the other hand, the thermal current is not exponentially suppressed, but roughly follows a power-like decrease with $\Delta\varepsilon_d$. Therefore, breaking of the electron-hole symmetry is not as pronounced so that $S$ remains small in the cotunneling region centered around $\varepsilon_d^*$.

## 7.5 Summary

Using a model for electronic transport through a single spin-degenerate molecular orbital, and taking into account oscillational and vibrational phonons, we have calculated the thermopower of a single-molecule device in the regime of weak molecule-lead coupling. In contrast to $IV$ measurements, the thermopower provides a means of extracting information about electronic and phononic excitations, and about the nature of the electron-phonon coupling in a linear response measurement. Therefore, it may have advantages over the more conventional $IV$ characteristic, which necessarily involves nonequilibrium effects, and which, at large voltages, may even affect symmetry and structure of the molecule itself. In addition, the sign of the thermopower signals the breaking of particle-hole symmetry and thus allows one to determine whether transport proceeds by tunneling through the HOMO or LUMO.

We have found that sequential-tunneling contributions yield a characteristic sawtooth behavior of the thermopower as a function of gate voltage for low temperatures, which shows structure due to electronic and phononic excitations. It has been shown that due to the different nature of electron-phonon coupling for oscillations and vibrations, characteristic differences in the phonon step size arise in the sequential-tunneling thermopower. Analytical expressions for the phonon step size have been derived in the limit of strong Coulomb blockade, which show that, for realistic parameters, phonon steps can be expected to be more pronounced for vibrations than for oscillations.

Away from the Coulomb peaks, cotunneling dominates over sequential tunneling. By considering these cotunneling contributions, we have found that the (elastic) cotunneling regime does not show significant structure due to phononic excitations. We have investigated the crossover regime and have given an estimate for the gate voltage at which the crossover takes place. It has been shown that the phononic structure exhibited by the sequential-tunneling contributions is retained in the thermopower if $k_B T \ll \hbar\omega_0$ and $k_B T \ln \alpha^{-1} > \hbar\omega_0$, i.e., (1) the temperature is low enough so that the phononic structure is not blurred out,

and (2) the dimensionless coupling parameter $\alpha$ is so small that the crossover gate voltage is high enough to allow for at least one phonon feature in the thermopower.